FOCUS ISSUE OF SELECTED PAPERS FROM IMLB 2016 WITH INVITED PAPERS CELEBRATING 25 YEARS OF LITHIUM ION BATTERIES

Effective Suppression of Polysulfide Dissolution by Uniformly Transfer-Printed Conducting Polymer on Sulfur Cathode for Li-S Batteries

San Moon,[a,b,=] Jung-Keun Yoo,[a,c,=] Young Hwa Jung,[a,d,*] Joo-Hyung Kim,[a] Yeon Sik Jung,[a,z] and Do Kyung Kim[a,z]

[a]*Department of Materials Science and Engineering, Korea Advanced Institute of Science and Technology (KAIST), Daejeon 34141, Korea*
[b]*Samsung Advanced Institute of Technology (SAIT), Suwon 16678, Korea*
[c]*LG Chem, Daejeon 34122, Korea*
[d]*Pohang Accelerator Laboratory (PAL), Pohang, Gyeongbuk 37673, Korea*

The lithium-sulfur battery has received much attention in recent years owing to its high gravimetric capacity, far beyond that of current Li-ion batteries. Overcoming the shuttling effect caused by the dissolution of polysulfides during the charge-discharge process is a major challenge for the realization of Li-S cells. Here we report transfer-printing of a conductive polymer to cover and securely passivate the surface of sulfur electrodes to prevent the dissolution of polysulfides and, simultaneously, to provide high electronic conductivity of sulfur cathodes. Highly uniform polyaniline film can be controllably formed on sulfur cathodes via the transfer printing method, and a sulfur cathode with the printed polyaniline layer showed improved cycle performance (capacity retention of 96.4% and an average Coulombic efficiency of 99.6% for 200 cycles) compared to conventional sulfur cathodes. In situ measurement of transmittance during discharge demonstrated that the dissolution of sulfur in electrolytes is considerably suppressed by the printed polyaniline layer, substantiating that transfer-printed polyaniline film can provide robust protection as well as supplement electrical conductivity to the sulfur cathode. This strategy could be extensively applied to sulfur cathodes of diverse morphology and further extended to large-scale production.

Manuscript submitted October 19, 2016; revised manuscript received January 9, 2017. Published January 25, 2017. This was Paper 1191 presented at the Chicago, Illinois, Meeting of the IMLB, June 19–24, 2016. *This paper is part of the Focus Issue of Selected Papers from IMLB 2016 with Invited Papers Celebrating 25 Years of Lithium Ion Batteries.*

The development of high-energy density rechargeable batteries is of great significance, given the continuously increasing demand for portable electronic devices, and for a variety of electric vehicles (EVs).[1–6] However, the energy density of commercial lithium-ion batteries, which are based on lithium intercalation oxides and graphite, is limited to about 150 Wh kg^{-1}, still far from what is needed for practical EVs. This is chiefly due to the heavy weight and insufficient storage capacity of transition-metal insertion compounds (e.g., $LiCoO_2$, $LiMn_2O_4$, and $LiFePO_4$).[7,8] As an alternative material for light-weight cathodes, sulfur can react with metallic lithium to form Li_2S via a two-electron reaction, leading to a high theoretical capacity of 1675 mAh g^{-1} and a high theoretical energy density of 2500 Wh kg^{-1} in lithium-sulfur battery systems. This is almost an order-of-magnitude higher than that of conventional Li-ion batteries.[9,10] Moreover, the natural abundance, low cost, and environmental friendliness of sulfur could make lithium-sulfur materials highly practical for next generation, high-energy-density batteries.

However, the practical application of Li-S cells is still challenging, mainly due to their high volumetric expansion and shrinkage (up to 80%), to the dissolution of polysulfides resulting in the so-called shuttling mechanism during the charge-discharge process, and due to the low electronic conductivity of sulfur ($\sim 10^{-30}$ S cm^{-1}).[11–13] In particular, the polysulfide shuttling mechanism is caused by the phenomenon that, during a charge cycle, dissolved polysulfides in electrolytes diffuse to the Li anode, are reduced; then diffuse back to the sulfur cathode during discharge cycles as they consume the active materials.[14–17] These challenges must be met to enable more extensive, practical utilization of lithium-sulfur batteries.

Considerable efforts have been made to enhance the electrochemical performance of sulfur cathodes for more advanced lithium-sulfur cells. One of the most effective approaches is the encapsulation of sulfur particles in a conducting matrix to improve electrical conductivity, and to prevent the dissolution of high-order polysulfides.[18,19] For example, mesoporous carbon was used to trap high-order polysulfides in their small, numerous pores.[20] However, despite the successful improvement of electrochemical performance, the weight fraction of the sulfur in these composite electrodes is usually low (<50%), resulting in a loss of total energy density in the cell.[21,22] Other approaches that achieved relatively higher sulfur content inevitably involved a complicated process for scaling up lithium-sulfur cells.[23]

To address these important issues, here we report transfer-printing of conductive polymer (polyaniline) to cover and securely passivate the surface of sulfur electrodes to prevent the dissolution of polysulfides and, simultaneously, to provide high electronic conductivity of sulfur cathodes. As a result, the trapping effect of polysulfides by the uniformly printed thin polyaniline, enhanced cycling stability substantially. The capacity retention was 96.4% with an average Coulombic efficiency of 99.6% during 200 cycles, which is markedly improved compared to a bare counterpart. Moreover, unlike previous approaches, our printing method could be widely applied to the diverse morphology of sulfur cathodes and could be extended to large-scale production.

Experimental

Preparation of the graphene oxide-sulfur composite (GO-S).— All chemicals used in the synthesis of graphene oxide were purchased from Sigma Aldrich. Graphene oxide (GO) was prepared using a modified Hummer's method. After washing and exfoliating the GO samples, the centrifuged GO was freeze-dried under vacuum for two days. The graphene oxide (GO) and sulfur (Sigma Aldrich) (weight ratio of 1:3) were mixed by ball milling. The mixture was heated at

=These authors contributed equally to this work.
*Electrochemical Society Member.
zE-mail: ysjung@kaist.ac.kr; dkkim@kaist.ac.kr

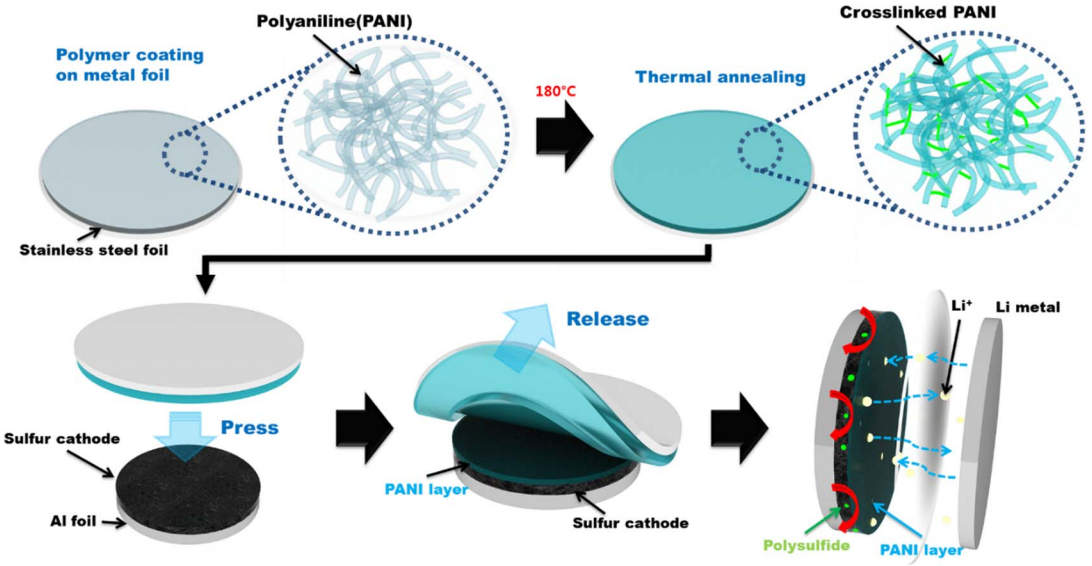

Figure 1. Schematic illustration of the PANI-layer coated by a printing method.

155°C for 12 h in a closed vessel for sulfur infiltration.[24] The sulfur content of GO-S composite is about 74%, which is about the same as the initial GO and sulfur ratio.

Preparation of polyaniline (PANI).—The aniline monomer solution (Sigma Aldrich) was mixed with 1 M hydrochloric acid (HCl) (Sigma Aldrich) in a volume ratio of 100:1 under stirring. After 30 min, the equivalent number of moles (with respect to aniline) of 22.8 wt% aqueous ammonium persulfate solution (APS) (Sigma Aldrich) was slowly added, followed by oxidative polymerization at 0°C for 24 h. The resultant green solid was obtained by centrifugation and washed thoroughly with water and ethanol, to remove excess ions and monomers.

Preparation of the PANI-printed electrode.—To prepare working electrodes, the as-prepared GO-S was mixed with the conducting carbon Super P (Timcal) and the binder sodium alginate (Sigma Aldrich) in a weight ratio of 75:15:10 using an agate mortar to the DI-water. The slurry thus prepared was cast on an aluminum foil (UACJ) and dried at 60°C under vacuum for 24 h. The PANI solution in n-methyl-2-pyrrolidone (NMP) (20 wt%) was spin-coated and tape-casted onto stainless steel foil. The polymer-coated substrate was annealed at 180°C for 1 h. The PANI layer was printed on top of the electrode surface using a roll press.

Preparation of the air-tight cell for UV/Vis measurement.—To measure the in situ UV/Vis transmittance spectra for the lithium-sulfur cell during discharge, the electrode was fixed on one side of a rectangular-tube cell using paraffin film, followed by placement of the Li metal (HONJO) on the opposite side. Then, the cell was completely filled with electrolyte and capped with polydimethylsiloxane (PDMS). All procedures were carried out in a glove box filled with high-purity Ar gas.

Characterization.—The weight fractions of carbon and sulfur were determined using an Elemental Analyzer (Flash 2000, Thermo Scientific). The morphology of the materials was observed using field-emission scanning electron microscopy (FESEM, Hitachi S-4800). The transmittance of the lithium-sulfur cell was measured by UV/Vis spectrometer (UV-3101PC, Shimadzu Co., Japan). The reflectance spectra were recorded using a spectral incident photon-to-current efficiency (IPCE) measurement system, equipped with an integrating sphere assembly (K3100, McScience, Korea).

Cell assembly and battery testing.—Electrochemical measurements of all electrodes were performed by preparing 2032-type coin cells that were assembled in an Ar-filled glove box. The PANI-printed electrode and lithium foil were used as the working and counter/reference electrodes, respectively. The electrolyte was prepared by dissolving 1 M lithium bis(trifluoromethanesulfonyl)imide (LiTFSI) (Sigma Aldrich) in a solvents of 1,3-dioxolane (anhydrous, contains ~75 ppm BHT as an inhibitor, 99.8%, Sigma-Aldrich) and 1,2-dimethoxyethane (anhydrous, 99.5%, Sigma-Aldrich) (volume ratio = 1:1). Before the electrolyte preparation, these solvents were stored over molecular sieves for 24 h to remove moisture. Polypropylene membranes (Celgard, Inc.) were used as separators. Galvanostatic measurements were performed in the potential range of 1.0 to 3.0 V vs. Li^+/Li using a battery cycler (WBCS3000, WonAtech). The C-rates for all coin cells were calculated based on the theoretical capacity of sulfur in the composite, for which 1 C is 1675 mA g^{-1}. The mass of sulfur loaded as the active material is about 5 mg cm^{-2}. All of the electrochemical measurements were performed at 25°C. For the in-situ UV/Vis measurement, the quartz cuvette cell was completely covered with the lid to avoid interference by ambient light. After taking the initial spectrum of the as-prepared cell, the Li-S cell was discharged at a rate of C/20 using a potentiostat (VSP-200, Bio Logic). Meanwhile, UV/Vis spectra were recorded every 0.1 V from the open-circuit-voltage (~2.8 V) to 1.5 V.

Results and Discussion

One of the key advantages of the transfer-printing method is that the polymer layer thickness and heat-treatment conditions are controllable without affecting the underlying electrodes. As schematically summarized in Figure 1, the PANI solution in NMP was spin-coated onto a stainless steel foil to obtain a thin, uniform film the thickness of which could be controlled by adjusting the solution concentration and spin-casting speed. The PANI-coated substrate was then annealed at 180°C for crosslinking.[21] It was expected that the cross-linked PANI layer would improve the trapping of polysulfides and play a role as a buffer layer against the volume changes of the sulfur electrode during repeated charge-discharge cycles. Then, the PANI layer was transfer-printed on top of the sulfur electrode via simple contact of the PANI-coated side of the stainless foil. Detailed procedures were described in the Experimental section.

The morphologies of the electrode with and without PANI coating are shown in Figure 2a. Figure 2a shows the rough surface of the pristine GO-S electrode, which is composed of GO-S, active

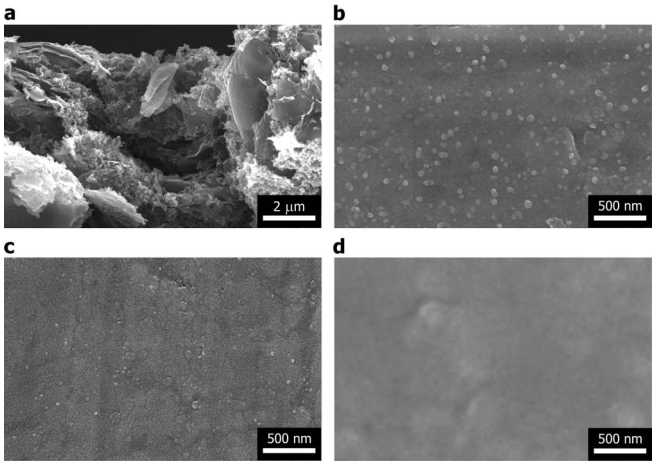

Figure 2. SEM images of (a) Unprinted electrode, (b) PANI-coated stainless-steel foil, (c) PANI-printed sulfur electrode, and (d) PANI-printed electrode; after 100 cycles.

carbon, and Na-alginate binder. The surface image of the PANI-coated stainless steel foil shown in Figure 2b, indicates the flat morphology of the conducting polymer thin film. As shown in Figure 2c, after transfer of the PANI layer onto the GO-S electrode, the flat PANI was homogeneously formed on the surface of the GO-S electrode. A sandwich structure of PANI membrane/active materials/Al foil can avoid not only the detachment of the active materials from the current collector, but also has the advantage of preventing the formation of high-order polysulfide and its diffusion to lithium metal, thus suppressing the shuttling mechanism to a great extent. Therefore, it is expected that both the cyclability and Coulombic efficiency of the Li-S cell could be improved. In order to examine the morphology changes after charge/discharge, a repeatedly cycled cell was disassembled in a glove box and washed thoroughly with propylene carbonate (PC) solvent. It can be seen from Figure 2d that, except for the formation of slight cracks, most of the PANI layer retained integrity after electrochemical cycling, implying the stability of the PANI layer during charge-discharge in the electrolyte.

The electrochemical performance of the PANI-printed electrode was evaluated using coin-type half-cells. Figure 3a shows the thickness of the PANI layers measured using a surface profiler. The thickness of spin-coated PANI layer was controlled (from 1 to 5 μm) by adjusting the spin casting speed from 1000–3000 r/min. For comparison, a tape-casted PANI layer with a thickness of 30 μm was also prepared. The mass of PANI layer with a thickness of 1 μm was about 0.1 mg. Then, we compared the galvanostatic capacity-voltage profiles of the sulfur electrodes containing different types of PANI protection layer. Figure 3b presents the second discharge-charge profiles during 0.1 and 1C cycling. It was found that there exist two plateaus, at approximately 2.3 and 2.0 V, for bare sulfur electrodes due to the two-step reduction of sulfur in the presence of Li ions.[24,25] On the other hand, the PANI-printed samples presented a large overpotential and decrease in capacity, due to the PANI capping layer.

However, the cycle performance test results in galvanostatic mode showed that the PANI-covered electrode presented both significantly

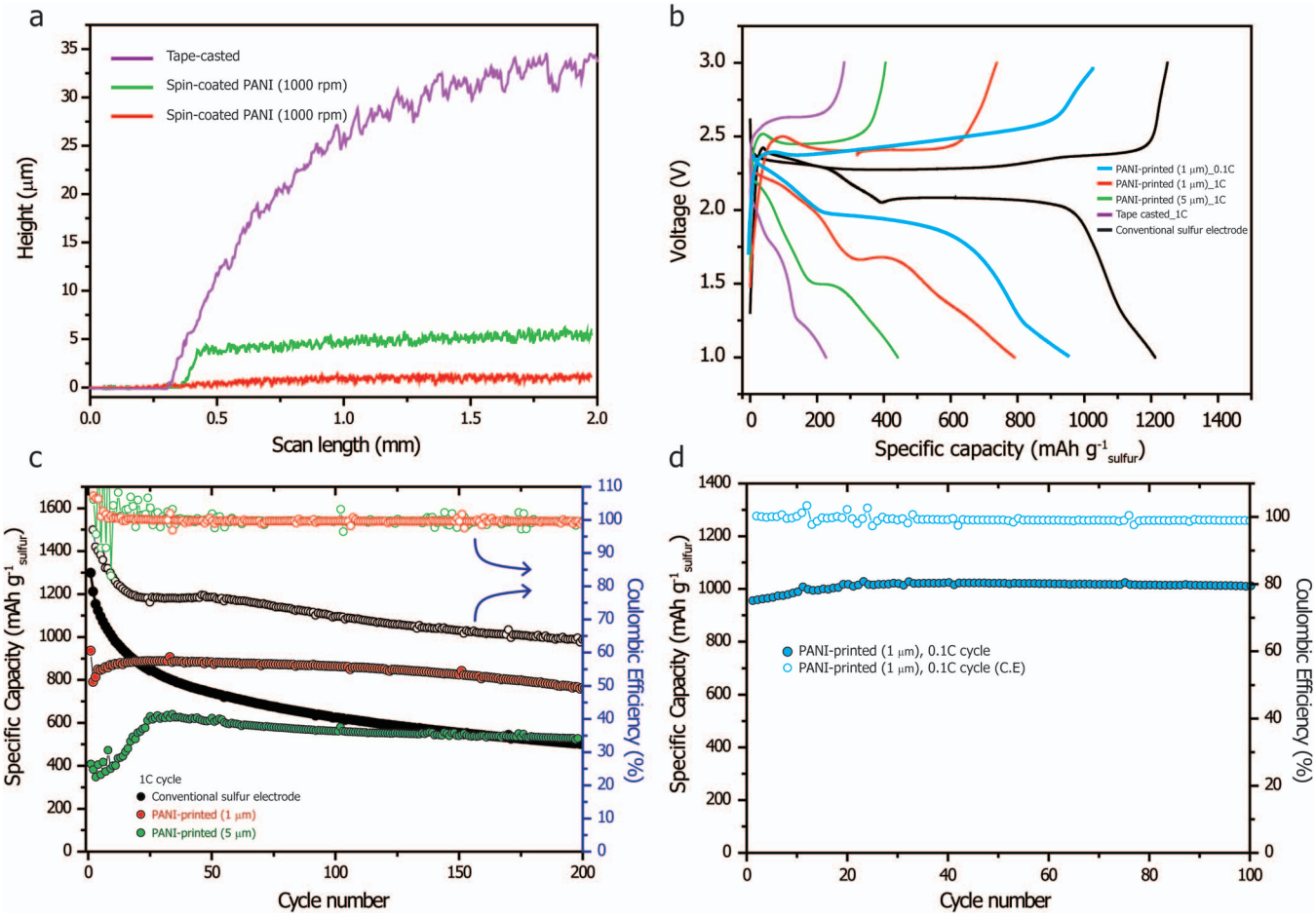

Figure 3. (a) Thickness of the PANI layer, (b) Galvanostatic capacity-voltage profiles of the sulfur electrodes (1 C = 1675 mA g^{-1}), (c) Capacity retention and Coulombic efficiency of the sulfur electrodes at 1 C-rate, (d) Cycle performance of the PANI-printed electrode with a 1 μm PANI layer at the rate of 0.1C.

improved cyclability and high Coulombic efficiency. Whereas the conventional sulfur electrode delivered an initial discharge capacity of 1298 mAh g^{-1}, the retained capacity was only 500 mAh g^{-1} (41.2% retention with respect to the capacity in the second cycle) after 200 cycles at a rate of 1C (Figure 3c). The average Coulombic efficiency of the conventional sulfur electrode in the cycle range 2–200 was low (∼ 71.6%). The PANI-printed cell with a 5-μm PANI layer initially delivered 400 mAh g^{-1} (discharge capacity), but this capacity increased to 600 mAh g^{-1} after 50 cycles. Interestingly, the Coulombic efficiency of the cell with the PANI-printed layer showed significant improvement (close to 100%) compared with the conventional sulfur electrode. In the case of printed cells with a 1 μm PANI protection layer, despite a relatively lower initial discharge capacity (935 mAh g^{-1}), the capacity retention (96.4%) was markedly higher, with an average Coulombic efficiency of 99.6%.

To confirm the cyclability with a low C-rate, the cycle performance of the PANI-printed cell with a 1-μm PANI layer was further evaluated at 0.1C for 100 cycles (Figure 3d). Even when the operation time for a cycle was increased 10-fold from 1C to 0.1C, 105% of the original capacity was still retained, with 99.3% of average Coulombic efficiency. The galvanostatic capacity-voltage profile of the PANI-printed cell with a 1-μm PANI layer was also shown in Fig. S1. This can be attributed to the fact that the PANI layer printed onto the electrode surface effectively prevented the dissolution of the polysulfides. However, it was also found that the printing of thicker PANI layers (1 and 5 μm) caused much lower capacity values (Figure 3b). This phenomenon implies that there exists an optimal range of PANI-layer thickness, because a too thick layer would hinder the diffusion of Li ions, while a too thin layer could not function as a robust blocking layer. Electrochemical impedance spectroscopy (EIS) was measured between 100 mHz and 1 MHz at the open circuit potential of the cell with a signal peak-to-peak amplitude of 5 mV for the samples with conventional sulfur electrode and PANI-printed (1 and 5 μm) as shown in Fig. S2. As the PANI layer becomes thicker, the second semicircle in a low frequency region become apparent and all the charge transfer resistance (R_{ct}) values increase.

In order to verify the hypothesis that the outstanding capacity retention and Coulombic efficiency of the PANI-printed electrode is due to the suppression of sulfur dissolution, in situ UV-Vis tests were performed with beaker-type cells. The cells were designed to allow the penetration of the beam from the UV/Vis spectrometer, and the sulfur cathode and the Li-metal anode were fixed on opposite sides of the cell to avoid interference from the ambient light. In Figure 4b, the UV spectrum of the conventional bare electrode showed almost 100% of transmittance at the open circuit voltage. During the discharge cycle, however, a significant change of transmittance spectra (Δ T ∼ 21.1% at the wavelength of 605 nm at 2.1 V) was observed, indicating serious dissolution of the long-chain polysulfides in the electrolytes. However, the PANI-printed sample showed much less change in the transmittance (Δ T < 10%) during the entire discharge process, as confirmed in Figure 4c. These results are consistent with the excellent cyclability provided by the PANI protection layer, which prevents the polysulfides from shuttling during the electrochemical reactions in the cell.

Conclusions

To summarize, we demonstrated that the formation of a conducting polymer protection layer could resolve the chronic polysulfide shuttling issue occurring in conventional Li-S batteries. We showed that a very uniform PANI film could be controllably formed on sulfur cathode via the transfer printing method, with outstanding manufacturability, scalability, and cost-effectiveness. The effectiveness of the printed conducting polymer layer was confirmed by improved cycle performances (capacity retention of 96.4% and an average Coulombic efficiency of 99.6% for 200 cycles) compared to conventional sulfur electrodes (poor retention of ∼ 41%). In situ transmittance measurement during discharge demonstrated that the dissolution of sulfur in electrolytes could be substantially suppressed by the printed PANI layer, substantiating that transfer-printed PANI film can provide robust protection as well as supplement electrical conductivity to the sulfur cathode. We expect that the strategy proposed in this work could be extensively applied for a variety of other energy-storage electrodes that require both secure protection and electrical conductivity during repeated charge-discharge cycles.

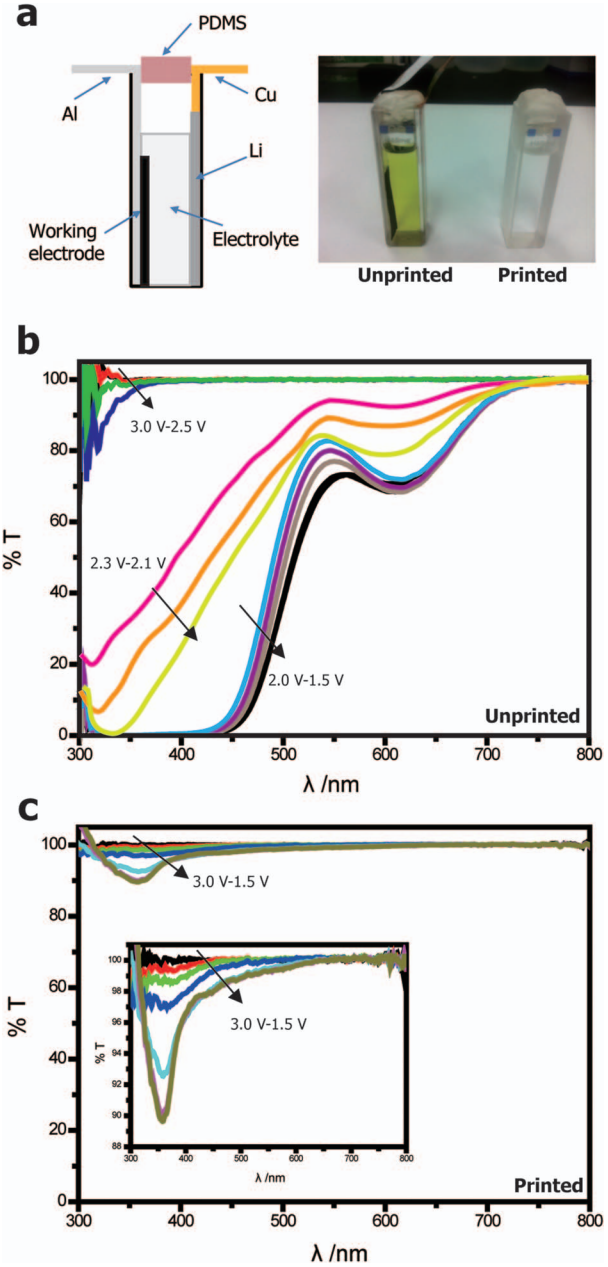

Figure 4. (a) Schematic illustration of UV/Vis measurement and photos after the test, UV/Vis spectra measured in operando mode during first discharge of (b) Unprinted and (c) Printed electrode.

Acknowledgment

This work was supported by the Climate Change Research Hub of KAIST (grant No. N11160019).

References

1. M. Armand and J. M. Tarascon, *Nature*, **451**(7179), 652 (2008).
2. J. B. Goodenough and Y. Kim, *Chem Mater*, **22**(3), 587 (2010).
3. B. Scrosati, J. Hassoun, and Y. K. Sun, *Energ Environ Sci*, **4**(9), 3287 (2011).

4. P. G. Bruce, S. A. Freunberger, L. J. Hardwick, and J. M. Tarascon, *Nat Mater*, **11**(2), (2012).
5. M. S. Whittingham, *Chem Rev*, **104**(10), 4271 (2004).
6. C. Liu, F. Li, L. P. Ma, and H. M. Cheng, *Adv Mater*, **22**(8), E28 (2010).
7. S. Y. Chung, J. T. Bloking, and Y. M. Chiang, *Nat Mater*, **1**(2), 123 (2002).
8. A. Manthiram, *J Phys Chem Lett*, **2**(3), 176 (2011).
9. N. Jayaprakash, J. Shen, S. S. Moganty, A. Corona, and L. A. Archer, *Angew Chem Int Ed Engl*, **50**(26), 5904 (2011).
10. X. L. Ji and L. F. Nazar, *J Mater Chem*, **20**(44), 9821 (2010).
11. C. D. Liang, N. J. Dudney, and J. Y. Howe, *Chem Mater*, **21**(19), 4724 (2009).
12. F. Wu, J. Z. Chen, R. J. Chen, S. X. Wu, L. Li, S. Chen, and T. Zhao, *J Phys Chem C*, **115**(13), 6057 (2011).
13. Y. Z. Fu and A. Manthiram, *Rsc Adv*, **2**(14), 5927 (2012).
14. H. Yamin, A. Gorenshtein, J. Penciner, Y. Sternberg, and E. Peled, *J Electrochem Soc*, **135**(5), 1045 (1988).
15. D. Aurbach, E. Pollak, R. Elazari, G. Salitra, C. S. Kelley, and J. Affinito, *J Electrochem Soc*, **156**(8), A694 (2009).
16. C. Barchasz, J. C. Lepretre, F. Alloin, and S. Patoux, *J Power Sources*, **199**, 322 (2012).
17. L. Suo, Y. S. Hu, H. Li, M. Armand, and L. Chen, *Nat Commun*, **4**, 1481 (2013).
18. X. Ji, K. T. Lee, and L. F. Nazar, *Nat Mater*, **8**(6), 500 (2009).
19. G. Zheng, Y. Yang, J. J. Cha, S. S. Hong, and Y. Cui, *Nano Lett*, **11**(10), 4462 (2011).
20. X. L. Li, Y. L. Cao, W. Qi, L. V. Saraf, J. Xiao, Z. M. Nie, J. Mietek, J. G. Zhang, B. Schwenzer, and J. Liu, *J Mater Chem*, **21**(41), 16603, (2011)
21. J. Z. Wang, L. Lu, M. Choucair, J. A. Stride, X. Xu, and H. K. Liu, *J Power Sources*, **196**(16), 7030, (2011).
22. L. C. Yin, J. L. Wang, F. J. Lin, J. Yang, and Y. Nuli, *Energ Environ Sci*, **5**(5), 6966, (2012).
23. S. Moon, Y. H. Jung, W. K. Jung, D. S. Jung, J. W. Choi, and D. K. Kim, *Adv Mater*, **25**(45), 6547 (2013).
24. S. Moon, Y. H. Jung, and D. K. Kim, *J Power Sources*, **294**, 386 (2015).
25. S. Xin, L. Gu, N. H. Zhao, Y. X. Yin, L. J. Zhou, Y. G. Guo, and L. J. Wan, *J Am Chem Soc*, **134**(45), 18510 (2012).